Structural Chemistry
https://doi.org/10.1007/s11224-018-1228-8

ORIGINAL RESEARCH

The electronic structure, solvatochromism, and electric dipole moments of new Schiff base derivatives using absorbance and fluorescence spectra

Yadigar Gülseven Sıdır[1] · Cebrail Aslan[2] · Halil Berber[3] · İsa Sıdır[1]

Received: 9 August 2018 / Accepted: 2 November 2018

Abstract
The electronic structure and electronic transitions of four new mono Schiff base derivatives are interpreted by using absorption and fluorescence spectra including 28 different solution medium. Electrical dipole moments have been found by means of four different quantum mechanical methods based on solvatochromic shifts like Lippert–Mataga, Bakhshiev, modified Bilot–Kawski, and Reichardt methods. Quantitative researches of solvent-solute interactions are done by using Kamlet–Taft and Catalan parameters. In absorption and fluorescence spectra, bathochromic shift occurs with dispersion-polarization forces effect. The electronic transitions and electronic structure of these molecules have changed to dependent on solvent medium property. HOMO, LUMO, MEP, and SAS were calculated using B3LYP/6-311G(d,p) level of theory. Solvatochromism, photophysical properties, and electronic structure were discussed in detail. The dipole moments in ground-state and excited-state have not almost change.

Keywords Kamlet-Taft solvatochromism · Catalan solvatochromism · Electrical dipole moment · Electronic transitions · Photophysical properties · Schiff bases

Introduction

Schiff bases are compounds containing the azomethine group (–RC = N–) and are usually compounds in which the primary amine occurs as a result of condensation reaction with an active carbonyl. There are a number of studies on compounds known as Schiff bases [1–5]. These compounds have a lot of usage areas and are still an intensive research topic, whether having novel and fresh usage areas, because the electronic and molecular structure of Schiff bases and compounds having Schiff bases nucleus have own. The more interesting usage areas from Schiff bases compounds and complex are biological activity such as anticancer, antioxidant [6–8], antiviral [9–11], antifungal [12–14], antibacterial [15, 16], antimicrobial [17–19], genotoxic [20], and antiproliferative properties [21–24]. The Schiff bases like push-pull systems have very different properties such as organic photovoltaic materials [25, 26], membrane sensors [27–34], non-linear optic materials [35–39], chemosensor properties [40–45], photochromism properties [46–48], optical switching devices [49], solvatochromic properties [50–55], fluorescent materials [56, 57], and liquid crystal properties [58–60]. Thus, electronic structures of these group molecules and novel derivatives need to be examined in detail.

The electric dipole moments of molecules are very important from physical parameters due to the dipole moment values that provide information about the change in the electronic distribution and electronic change during excitation. The most common method used experimentally to determine electric dipole moments is quantum mechanical method done with using solvatochromic shifts in spectrums. The dipole moments are

Electronic supplementary material The online version of this article (https://doi.org/10.1007/s11224-018-1228-8) contains supplementary material, which is available to authorized users.

✉ Yadigar Gülseven Sıdır
ygsidir@beu.edu.tr; yadigar.gulseven@gmail.com

[1] Department of Physics, Faculty of Arts and Science, Bitlis Eren University, 13000 Bitlis, Turkey

[2] Department of Physics, Science Institute, Bitlis Eren University, 13000 Bitlis, Turkey

[3] Department of Chemistry, Faculty of Science, Anadolu University, 26470 Eskişehir, Turkey

Published online: 22 November 2018

calculated using Lippert–Mataga [61, 62], Bakhshiev [63], Reichardt [64], and modified Bilot–Kawski [65–71] methods. Solvatochromism has researched to changes in the electronic structures of molecules depending on their solvent environment. Compounds having solvatochromic properties are molecules that can be used during organic electronics, optical switching, and processes in which electrons actively act. The statistical analysis of solvatochromism, in that, another name is LSERs (linear solvation energy relationships), done using Kamlet–Taft [72, 73] and Catalan parameters [75–77], and physical and solution parameters done on solvent-solute interactions in different medium during excitation could be calculated to qualitative effects [77, 78].

Thus, it must be determined in Schiff bases and their derivatives. In this study, the electronic structure, solvatochromism, and electric dipole moment of four new Schiff base molecules titled as (E)-2-(2,5-dimethoxybenzylideneamino)phenol (S1), (E)-4-(3,4-dimethoxybenzylideneamino)phenol (S2), (E)-N-(2,4-dimethoxybenzyliden)benzeneamine (S3), and (E)-4-(2,4-dimethoxybenzylideneamino)phenol (S4) molecules were determined after these molecules were synthesized and characterized. The absorbance (UV) and fluorescence spectra of Schiff base derivatives were measured at room temperature in 28 different solvents with different polarities. Solvent-solute interactions of the molecules are analyzed by using Kamlet–Taft and Catalan solvatochromism, which are LSER models. Using the values obtained from the Kamlet–Taft and Catalan solvatochromism, the quantities involved in solvent-solute interactions such as solvent polarity, solvent dipolarity, solvent acidity, and solvent basicity, dispersion-induction interaction, and dipolar-orientation interaction were compared with each other. The excited- and ground-state electric dipole moments are calculated by the methods of Lippert–Mataga, Bakhshiev, modified Bilot–Kawski, and Reichardt, respectively. Ground-state and excited-state dipole moments, HOMO, LUMO, SAS, and MEP shape, have been calculated by using DFT (B3LYP) method and 6-311G(d,p) basis set in gas phase.

Materials and methods

Materials

The solvents and molecules were purchased from Sigma-Aldrich. They were used without purification.

Synthesis method

The synthesis method of Schiff bases is given in supplementary materials. We show the synthesis reaction scheme in Fig. 1. The ^{13}C NMR, ^{1}H NMR, and FT-IR spectra of synthesized novel Schiff base compounds are shown in Figs. 1S–4S.

Synthesis of 2-((2,5-dimethoxybenzylidene)amino)phenol (S1)

2-Aminophenol (1.091 g (0.01 mol)) was dissolved gently in 25 mL of MeOH to complete dissolution of the material. To this solution, 1.661 g (0.01 mol) of 2,5-dimethoxybenzaldehyde solution in 25 mL of MeOH was slowly added with stirring. The crude product was filtered and purified by recrystallization from methyl alcohol, and the vacuum was dried in a desiccator.

IR (KBr, disc, ν cm^{-1}): 3375 (O–H), 3304–3000 (C–H, aromatic), 2957–2834 (C–H, aliphatic), 1591 (C=N), 1495–1379 (C=C, aromatic), 1222 (C–O, aromatic). ^{1}H NMR (300 MHz, DMSO) δ 9.01 (s, 1H), 8.94 (s, 1H), 7.80 (s, 1H), 7.13 (m, 1H), 7.08 (s, 1H), 7.08 (s, 1H), 6.92 (m, 1H), 6.88 (m, 1H), 6.85 (m, 1H), 3.84 (s, 2H), 3.80 (s, 3H). ^{13}C NMR (75 MHz, DMSO) δ 163.44 (s), 154.49 (s), 153.72 (s), 151.58 (s), 144.46 (s), 127.77 (s), 125.14 (s), 120.03 (s), 119.73 (s), 119.55 (s), 116.88 (s), 116.49 (s), 113.82 (s), 56.71 (s), 56.05 (s). Elemental analysis; $C_{15}H_{15}NO_3$, calculated (founded); C, 70.02 (64.04); H, 5.88 (5.83); N, 5.44 (5.28).

Synthesis of 2-((2,5-dimethoxybenzylidene)amino)phenol (S2)

Aminophenol 1.091 g (0.01 mol) was dissolved gently in 25 mL of MeOH to complete dissolution of the material. To this solution, 1.661 g (0.01 mol) of 3,4-dimethoxybenzaldehyde solution in 25 mL of MeOH was slowly added with stirring. The crude product was filtered and purified by recrystallization from methyl alcohol, and the vacuum was dried in a desiccator.

IR (KBr, disc, ν cm^{-1}): 3340 (O–H), 3004–2931 (C–H, aromatic), 2840–2604 (C–H, alifatik), 1618 (C=N), 1514–1419 (C=C, aromatic), 1272 (C–O, aromatic). ^{1}H NMR (300 MHz, DMSO) δ 9.44 (s, 1H), 8.49 (s, 1H), 7.52 (d, J = 1.8 Hz, 1H), 7.39 (d, J = 8.3, 1.8 Hz, 1H), 7.15 (dd, J = 8.7 Hz, 2H), 7.06 (d, J = 8.3 Hz, 1H), 6.79 (dd, J = 8.7 Hz, 2H), 3.83 (s, 4H), 3.82 (s, 2H). ^{13}C NMR (75 MHz, DMSO) δ 157.36 (s), 156.33 (s), 151.80 (s), 149.44 (s), 143.42 (s), 129.95 (s), 123.84 (s), 122.71 (s), 116.13 (s), 111.74 (s), 109.58 (s), 56.05 (s), 55.87 (s). Elemental analysis; $C_{15}H_{15}NO_3$, calculated (founded); C, 70.02 (78.59); H, 5.88 (5.85); N, 5.44 (4.70).

Synthesis of 1-(2,4-dimethoxyphenyl)-N-phenylmethanimine (S3)

Aniline 0.931 g (0.01 mol) was dissolved gently in 25 mL of MeOH to complete dissolution of the material. To this solution, 1.661 g (0.01 mol) of 2,4-dimethoxybenzaldehydesolution in 25 mL of MeOH was slowly added with stirring. The crude product was filtered and purified by recrystallization from methyl alcohol, and the vacuum was dried in a desiccator.

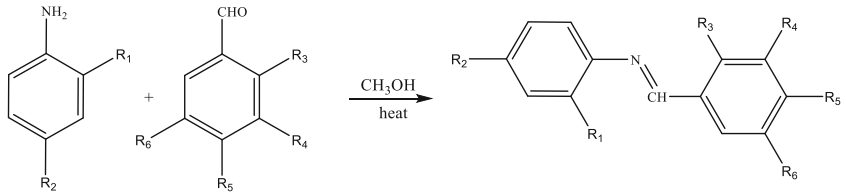

Fig. 1 The general synthesis reaction of Schiff bases compounds. $R_1 = OH$, $R_2 = H$, $R_3 = OCH_3$, $R_4 = H$, $R_5 = H$, $R_6 = OCH_3$, (E)-2-((2,5-dimethoxybenzylidene)amino)phenol (S1); $R_1 = H$, $R_2 = OH$, $R_3 = H$, $R_4 = OCH_3$, $R_5 = OCH_3$, $R_6 = H$, (E)-4-((3,4-dimethoxybenzylidene)amino)phenol (S2); $R_1 = H$, $R_2 = H$, $R_3 = OCH_3$, $R_4 = H$, $R_5 = OH_3$, $R_6 = H$, (E)-1-(2,4-dimethoxyphenyl)-N-phenylmethanimine (S3); $R_1 = H$, $R_2 = OH$, $R_3 = OCH_3$, $R_4 = H$, $R_5 = OH_3$, $R_6 = H$, (E)-4-((2,4-dimethoxybenzylidene)amino)phenol (S4)

IR (KBr, disc, ν cm^{-1}): 3017–2919 (C–H, aromatic), 2839–2572 (C–H, aliphatic), 1594 (C=N), 1506–1423 (C=C, aromatic), 1299 (C–O–C, aromatic). ^{1}H NMR (300 MHz, DMSO) δ 9.46 (s, 1H), 8.68 (s, 1H), 7.98 (d, $J = 20.0$, 8.3 Hz, 1H), 7.16 (t, $J = 7.9$ Hz, 1H), 6.60 (m, 5H), 3.88 (s, 3H), 3.85 (s, 3H). ^{13}C NMR (75 MHz, DMSO) δ 164.10 (s), 161.24 (s), 158.54 (s), 154.94 (s), 154.30 (s), 130.32 (s), 128.67 (s), 117.48 (s), 112.95 (s), 112.12 (s), 107.99 (s), 106.95 (s), 98.53 (s), 56.30 (s), 55.99 (s). Elemental analysis; $C_{15}H_{15}NO_3$, calculated (founded); C, 74.67 (54.70); H, 6.27 (4.09); N, 5.81 (4.69).

Synthesis of 4-((2,4-dimethoxybenzylidene)amino)phenol (S4)

4-Aminophenol 0.931 g (0.01 mol) was dissolved gently in 25 mL of MeOH to complete dissolution of the material. To this solution, 1.661 g (0.01 mol) of 2,4-dimethoxybenzaldehyde solution in 25 mL of MeOH was slowly added with stirring. The crude product was filtered and purified by recrystallization from methyl alcohol, and the vacuum was dried in a desiccator.

IR (KBr, disk, ν cm^{-1}): 3490 (O–H), 3053–2931 (C–H, aromatic), 2880–2583 (C–H, alifatik), 1609 (C=N), 1513–1448 (C=C, aromatic), 1278 (C–O, aromatic). ^{1}H NMR (300 MHz, DMSO) δ 9.40 (s, 1H), 8.72 (s, 1H), 7.94 (d, $J = 8.4$ Hz, 1H), 7.08 (d, $J = 8.6$ Hz, 2H), 6.78 (d, $J = 8.6$ Hz, 2H), 6.64 (s, 1H), 6.61 (s, 1H), 3.87 (s, 3H), 3.83 (s, 3H). ^{13}C NMR (75 MHz, DMSO) δ 163.61 (s), 160.86 (s), 156.17 (s), 152.26 (s), 144.22 (s), 128.31 (s), 122.54 (s), 117.95 (s), 116.16 (s), 106.80 (s), 98.53 (s), 56.24 (s), 55.93 (s). Elemental analysis; $C_{15}H_{15}NO_3$, calculated (founded); C, 70.02 (56.47); H, 70.02 (56.47); N, 5.44 (5.35).

Instruments and measurement methods

The ^{13}C NMR, ^{1}H NMR, and elemental analysis were done with using High-Resolution Digital 300 MHz Bruker Biospin NMR Spectrometer and LECO, CHNS-932 Elemental Analysis, respectively. FT-IR spectra were taken on a Perkin Elmer FT-IR Spectrometer. Ultraviolet–visible (UV–vis) absorption spectra and steady-state fluorescence spectra were recorded on Perkin Elmer Lambda-35 Spectrophotometer and Perkin Elmer-LS-55 Fluorescence Spectrometer, respectively The solutions were prepared as 5×10^{-5} M. Ultraviolet–visible absorption spectra were recorded on a wavelength range of 200–700 nm, when fluorescence spectra were recorded on by choosing excitation wavelength 340 nm for S1, 330 nm for S2, 330 nm for S3, and 340 nm for S4, respectively.

Electric dipole moment calculations

Lippert–Mataga, Bakhshiev, and Bilot–Kawski methods

The dipole moments were determined using the solvatochromic shifts. These methods are Lippert–Mataga (Eq. (1)) [61, 62], Bakhshiev (Eq. (2)) [63], and modified Bilot–Kawski (Eq. (3)) [65–70]. The theory of solvent-induced shifts was analyzed according to the formulas derived by Bilot and Kawski and rearranged by Chamma and Viallet [71].

$$\tilde{\nu}_a - \tilde{\nu}_f = m_1 F_1(\varepsilon, n) + \text{constant} \tag{1}$$

$$\tilde{\nu}_a - \tilde{\nu}_f = m_2 F_2(\varepsilon, n) + \text{constant} \tag{2}$$

$$\frac{\tilde{\nu}_a + \tilde{\nu}_f}{2} = -m_3 F_3(\varepsilon, n) + \text{constant} \tag{3}$$

Where

$$m_1 = \frac{2\left(\mu_e - \mu_g\right)^2}{hca_0^3} \tag{4}$$

$$m_2 = \frac{2\left(\mu_e - \mu_g\right)^2}{hca_0^3} \tag{5}$$

$$m_3 = \frac{2\left(\mu_e^2 - \mu_g^2\right)}{hca_0^3} \tag{6}$$

$\tilde{\nu}_a$ and $\tilde{\nu}_f$ are the absorption and fluorescence maxima wavenumbers (in cm^{-1}), respectively. $F_1(\varepsilon, n)$ (*Lippert − Mataga Function*), $F_2(\varepsilon, n)$ (*Bakshiev Function*), and $F_3(\varepsilon,$

n) (*Modified Bilot − Kawski Function*) are functions correlated given by Eqs. (7), (8), and (9), respectively; m_1, m_2, and m_3 are the slopes found by linear curve fitting as seen in Eqs. (7), (8), and (9), respectively.

$$F_1(\varepsilon,n)=\frac{\varepsilon-1}{2\varepsilon+1}-\frac{n^2-1}{2n^2+1} \tag{7}$$

$$F_2(\varepsilon,n)=\frac{2n^2+1}{n^2+1}\left[\frac{\varepsilon-1}{\varepsilon+2}-\frac{n^2-1}{n^2+2}\right] \tag{8}$$

$$F_3(\varepsilon,n)=\left[\frac{2n^2+1}{2(n^2+1)}\left(\frac{\varepsilon-1}{\varepsilon+2}-\frac{n^2-1}{n^2+2}\right)+\frac{3(n^4-1)}{2(n^2+2)^2}\right] \tag{9}$$

Here, ε and n are dielectric constant and refractive index of the solvents. Employing linear curve fitting route for $\tilde{\nu}_a-\tilde{\nu}_f$ versus $F_1(\varepsilon,n)$, $\tilde{\nu}_a-\tilde{\nu}_f$ versus $F_2(\varepsilon,n)$, and $\left(\tilde{\nu}_a+\tilde{\nu}_f\right)/2$ versus $F_3(\varepsilon,n)$ gives m_1, m_2, and m_3, respectively. If it can be supposed that ground- and excited-state dipole moments are parallel, then:

$$\mu_g=\frac{m_3-m_2}{2}\left(\frac{hca^3}{2m_2}\right)^{1/2} \tag{10}$$

$$\mu_e=\frac{m_3+m_2}{2}\left(\frac{hca^3}{2m_2}\right)^{1/2} \tag{11}$$

$$\mu_e=\frac{m_3+m_2}{m_3-m_2}\,\mu_g,(m_3>m_2) \tag{12}$$

Besides, the Reichardt method based on the empirical scale E_T^N [64, 77, 78] can be used for estimating dipole variation ($\Delta\mu$) from the solvatochromic shift. The theoretical basis for the correlation of the shift with E_T^N has been developed by Ravi et al. [79].

$$\tilde{\nu}_a-\tilde{\nu}_f=11307.6\left[\left(\frac{\nabla\mu}{\nabla\mu_B}\right)^2\left(\frac{a_B^B}{a_0}\right)^3\right]E_T^N+\text{constant} \tag{13}$$

Where $\Delta\mu_B=9D$ and $\alpha_B=6.2$ Å are the change in dipole moment on excitation and Onsager Radius of reference betaine dye, respectively. $\Delta\mu$ and α_0 have relevant with dipole moment change and Onsager radius for the solute molecule. The change in dipole moment $\Delta\mu$ and α_0 is the corresponding dipole moment change and Onsager radius for the solute molecule. The change in dipole moment $\Delta\mu$ can be determined as:

$$\mu_e-\mu_g=\sqrt{\frac{m_{E_T^N}\times 81}{11307.6\times\left({}^{6.2}/_{a_0}\right)^3}} \tag{14}$$

Where $m_{E_T^N}$ is the slope obtained from the linear plot of Stokes shift as indicated in Eq. (15).

$$\tilde{\nu}_a-\tilde{\nu}_f=m_{E_T^N}.E_T^N+\text{constant} \tag{15}$$

Quantum chemical calculations

Quantum chemical calculations are performed to research as detail to the electronic structure of the investigated molecule. Energy optimization and frequency calculations of this molecule have been done by using B3LYP/6-311G(d,p) [80] method and basis set with Gaussian09W software [81]. Frequency calculations have controlled to the question whether the imaginer frequency is observed or not. Afterwards, Onsager cavity radiuses of these molecules have been calculated by using B3LYP/6-311G(d,p) method and basis set. GaussView05 [82] is used for visualization of the results from the output file obtained from Gaussian09W.

Statistical methods

LSERs have depicted to the specific/nonspecific interactions and intra/inter molecular interactions in electronic transition mechanisms of solute molecules in the solvent medium. The LSER approach is preferable because it has been successfully applied to the positions or intensities of maximal absorption in UV–visible absorption and fluorescence spectra [77, 78]. The Kamlet–Taft solvatochromism equation is given as

$$\vartheta_{\max}=C_0+C_1f(n)+C_2f(\varepsilon)+C_3\beta+C_4\alpha \tag{16}$$

In here, $\vartheta_{\max}$ is defined as the maximum absorption band depending on solvent parameters of the molecule; $f(\varepsilon)=(\varepsilon-1)/(\varepsilon+1)$, $f(n)=(n^2-1)/(n^2+1)$, β, and α are determined as dipolarity-orientation and polarization-induction functions, hydrogen bonding acceptor ability, and hydrogen bonding donor ability, respectively. The C_0 coefficient can determine the maximum absorption band in gaseous phthe ase, and C_1, C_2, C_3, and C_4 are coefficients that represent $f(n)$, $f(\varepsilon)$, β, and α parameter values [72, 73].

Another method, Catalan solvatochromism equation, is given as [75–77].

$$\vartheta_{\max}=C_5+C_6SP+C_7SdP+C_8SA+C_9SB \tag{17}$$

In here, *SP* defines the solvent polarity, *SdP* defines solvent dipolarity, *SA* defines the acidity of solvent, and *SB* is the basicity of solvent. The C_5 coefficient can determine the

maximum absorption band in the gaseous phase. C_6, C_7, C_8, and C_9 are coefficients that represent *SP*, *SdP*, *SA*, and *SP* parameter values. Dielectric constant, ε, and refractive index, *n*, were taken from the literature [78].

Result and discussion

Electronic absorption and fluorescence spectra

The electronic spectral data of S1, S2, S3, and S4 in different non-polar, polar aprotic, and polar protic solvents with various polarities have been tabulated in Tables 1, 2, 3, and 4. As seen from Table 1 and Fig. 2, electronic absorption spectra of S1 molecule exhibit two main bands centered in the regions of 269–291 nm and 358.17–379.22 nm, respectively. These first electronic transition bands are born out from conjugations of aromatic rings, while second electronic transition bands are born out from delocalization between –N=CH– and aromatic rings. The second electronic band displays hypsochromic shifts in electronic absorption spectra with increasing solvent polarity.

Fluorescence spectra of S1 in different solvents are given in Fig. 2. As can be seen in Table 1 and Fig. 2, fluorescence spectra of S1 indicate three electronic transition bands in cyclohexane and two electronic transition bands in diethyl ether, n-butyl acetate, DCM, and acetonitrile and one electronic transition band in other solvents. The first band in the fluorescence spectra can be attributed to electronic transition of conjugation between –N=CH– and benzene ring. The second band in fluorescence spectra can be originated from the electron movements in the –N=CH– group. Fluorescence spectra wavelength λ_{PL}(nm), frequency ν (cm^{-1}), and Stokes shift values of S1 are listed in Table 1. Stokes shift does not regularly change with solvent polarity for S1.

The absorbance spectra of S2 in different solvents are given in Fig. 3. The absorbance spectra wavelength and wavenumber for S2 molecule are shown in Table 2. As can be seen in Table 2 and Fig. 4, electronic absorption spectra of S2 derivatives exhibit four

Table 1 The absorption and fluorescence wavenumber data in different solvent medium of S1 molecule

Solvents	λ_{abs}^{1}	λ_{abs}^{2}	ν_{abs}^{2}	λ_{PL}^{1}	ν_{PL}^{1}	λ_{PL}^{2}	λ_{PL}^{3}	λ_{PL}^{4}	ν_{abs}^{2}-ν_{PL}^{1}
n-Pentane	278.78	374.58	26,696.79	448.38	22,302.51	–	–	–	4394.28
n-Hexane	290.94	371.57	26,913.02	383.71	26,061.35	–	–	–	851.67
Cyclohexane	278.78	375.45	26,634.38	382.10	26,171.16	408.58	430.08	456.42	463.22
1,4-Dioxane	276.27	374.20	26,723.63	418.20	23,912	–	–	–	2811.63
Benzene	–	379.22	26,370.17	380.49	26,281.9	–	–	–	88.27
Toluene	–	377.96	26,457.66	382.69	26,130.81	–	–	–	326.85
o-Xylene	–	–	–	382.69	26,130.81	–	–	–	–
Diethyl ether	295.71	369.18	27,086.69	410.19	24,378.95	430.08	–	–	2707.74
Chloroform	278.78	376.71	26,545.73	437.25	22,870.21	–	–	–	3675.52
Ethyl acetate	288.81	370.44	26,995.01	426.72	23,434.57	–	–	–	3560.44
n-Butyl acetate	290.06	372.95	26,813.48	387.07	25,835.12	411.80	–	–	978.36
THF	–	368.06	27,169.75	430.08	23,251.49	–	–	–	3918.26
DCM	290.19	375.08	26,661.09	418.38	23,901.72	436.67	–	–	2759.37
1-Octanol	290.19	365.17	27,384.32	411.80	24,283.63	–	–	–	3100.69
1-Heptanol	274.51	362.41	27,592.77	411.36	24,309.61	–	–	–	3283.16
1-Hexanol	271.76	359.53	27,814.11	411.36	24,309.61	–	–	–	3504.5
1-Butanol	284.42	362.41	27,592.77	448.22	22,310.47	–	–	–	5282.3
iso-Butanol	284.42	358.15	27,921.23	451.44	22,151.34	–	–	–	5769.89
2-Propanol	258.97	359.53	27,814.11	450.71	22,187.22	–	–	–	5626.89
Acetone	–	366.68	27,271.95	414.87	24,103.94	–	–	–	3168.01
1-Propanol	268.87	363.79	27,488.15	453.20	22,065.31	–	–	–	5422.84
Ethanol	283.04	356.77	28,029.17	651.13	15,357.92	–	–	–	12,671.25
Benzonitrile	–	370.94	26,958.51	398.63	25,085.92	–	–	–	1872.59
Methanol	270.25	360.91	27,707.81	461.39	21,673.64	–	–	–	6034.17
DMF	287.30	366.68	27,271.95	426.72	23,434.57	–	–	–	3837.38
Acetonitrile	290.19	368.06	27,169.75	389.85	25,650.89	436.67	–	–	1518.86
Ethylene glycol	288.68	358.15	27,921.23	479.53	20,853.75	–	–	–	7067.48
DMSO	–	365.17	27,384.32	422.04	23,694.44	–	–	–	3689.88

Table 2 The absorption and fluorescence wavenumber data in different solvent medium of S2 molecule

Solvents	λ_{abs}^{1}	λ_{abs}^{2}	λ_{abs}^{3}	ν_{abs}^{3}	λ_{abs}^{4}	λ_{PL}^{1}	ν_{pl}^{1}	ν_{abs}^{3}-ν_{PL}^{1}
n-Pentane	–	274.40	328.43	30,447.89	–	379.61	26,342.83	4105.06
n-Hexane	–	272.13	312.01	32,050.25	341.60	359.26	27,834.99	4215.26
Cyclohexane	–	273.51	313.01	31,947.86	335.71	359.43	27,821.83	4126.03
1,4-Dioxane	–	279.53	332.70	30,057.11	–	399.95	25,003.13	5053.98
Benzene	–	326.67	335.45	29,810.7	–	407.26	24,554.34	5256.36
Toluene	–	–	337.08	29,666.55	–	376.69	26,547.03	3119.52
o-Xylene	–	–	343.10	29,146.02	–	357.67	27,958.73	1187.29
Diethyl ether	–	282.41	334.20	29,922.2	–	405.51	24,660.3	5261.9
Chloroform	266.11	273.92	337.08	29,666.55	–	409.16	24,440.32	5226.23
Ethyl acetate	–	279.53	332.70	30,057.11	–	390.73	25,593.12	4463.99
n-Butyl acetate	–	280.91	334.20	29,922.2	–	388.83	25,718.18	4204.02
THF	–	279.53	338.59	29,534.24	–	407.70	24,527.84	5006.4
DCM	–	282.41	334.20	29,922.2	–	417.21	23,968.74	5953.46
1-Octanol	–	282.41	341.60	29,274	–	413.26	24,197.84	5076.16
1-Heptanol	–	273.51	341.60	29,274	–	405.51	24,660.3	4613.7
1-Hexanol	–	279.53	341.60	29,274	–	401.70	24,894.2	4379.8
1-Butanol	–	280.91	340.09	29,403.98	–	405.51	24,660.3	4743.68
iso-Butanol	–	280.91	341.60	29,274	–	394.39	25,355.61	3918.39
2-Propanol	–	280.91	337.08	29,666.55	–	410.92	24,335.64	5330.91
Acetone	227.74	280.91	332.70	30,057.11	–	414.72	24,112.65	5944.46
1-Propanol	–	280.91	338.59	29,534.24	–	379.61	26,342.83	3191.41
Ethanol	–	278.03	338.59	29,534.24	–	403.02	24,812.66	4721.58
Benzonitrile	–	316.39	337.08	29,666.55	–	394.39	25,355.61	4310.94
Methanol	224.73	282.41	340.09	29,403.98	–	405.36	24,669.43	4734.55
DMF	–	281.66	335.45	29,810.7	–	418.38	23,901.72	5908.98
Acetonitrile	227.74	281.66	332.57	30,068.86	–	418.38	23,901.72	6167.14
Ethylene glycol	227.74	281.66	339.72	29,436.01	–	398.19	25,113.64	4322.37
DMSO	–	–	334.48	29,897.15	–	398.05	25,122.47	4774.68

strong bands centered in the regions of 224–227 nm, 273–282 nm, 312–316 nm, and 328–341 nm, respectively. The first and second band in the fluorescence spectra can be originated to conjugation on benzene rings. The third band in the fluorescence spectra can be attributed to electronic transition due to delocalization between –N=CH– and benzene rings. The forth band corresponds to electronic transitions at –N=CH– group.

As can be seen in Table 2 and Fig. 3 in the fluorescence spectra of S2, it exhibits one band centered in the region of 357–418 nm. This band can be attributed to electronic emission transition that represents conjugation between –N=CH– and the benzene ring. As the polarity of the solvent increases, the wavelength increases irregularly and displays a bathochromic effect.

Absorbance spectra of S3 in different solvents are given in Fig. 4. The absorbance spectra wavelength wavenumbers for the S3 molecule are shown in Table 3. As can be seen in Table 3 and Fig. 4, absorbance spectra electronic transitions of S3 derivatives exhibit three strong bands centered in the regions of 231–240 nm, 267–280 nm, and 319–340 nm, respectively. The first and second band in the absorbance spectra can be attributed to electronic transition due to conjugation in benzene rings and conjugation between –N=CH– and benzene rings. The third band is originated from electronic transitions in –N=CH– group. As the polarity of the solvent increases, the wavelength decreases; in other words, it displays hypsochromic effect.

The fluorescence spectra of S3 in different solvents are given in Table 3 and Fig. 4. As can be seen in Table 3 and Fig. 4, the fluorescence spectra of S3 exhibit one band. This band can represent the florescence transitions that originated from conjugation between benzene ring and –N=CH– group. As the polarity of the solvent increases, the wavelength decreases irregularly and displays hypsochromic effect.

The absorbance spectra of S4 in different solvents are given in Fig. 5. The absorbance spectra wavelength and molar absorptivity values observed in for S4 molecule are shown in Table 4. As can be seen in Table 4 and Fig. 5, electronic absorption spectra of S4 derivatives exhibit four strong bands centered in the regions of 223–232 nm, 264–280 nm, 305–

Table 3 The absorption and fluorescence wavenumber data in different solvent medium of S3 molecule

Solvents	λ_{abs}^{1}	λ_{abs}^{2}	λ_{abs}^{3}	ν_{abs}^{3}	λ_{abs}^{4}	λ_{PL}	ν_{PL}	ν_{abs}^{3}-ν_{PL}
n-Pentane	–	267.75	312.15	32,035.88	334.90	422.04	23,694.44	8341.44
n-Hexane	–	268.19	300.44	33,284.52	–	369.52	27,062.13	6222.39
Cyclohexane	–	269.72	302.27	33,083.01	340.75	369.52	27,062.13	6020.88
1,4-Dioxane	–	274.18	329.04	30,391.44	–	403.02	24,812.66	5578.78
Benzene	–	–	333.80	29,958.06	–	434.03	23,039.88	6918.18
Toluene	–	–	320.71	31,180.82	–	374.35	26,712.97	4467.85
o-Xylene	–	315.95	343.38	29,122.26	–	374.35	26,712.97	2409.29
Diethyl ether	–	276.53	326.70	30,609.12	–	405.36	24,669.43	5939.69
Chloroform	–	278.94	331.46	30,169.55	–	417.21	23,968.74	6200.81
Ethyl acetate	–	274.18	319.54	31,294.99	–	419.70	23,826.54	7468.45
n-Butyl acetate	–	276.60	325.97	30,677.67	–	395.85	25,262.09	5415.58
THF	–	278.94	331.46	30,169.55	–	414.87	24,103.94	6065.61
DCM	–	272.94	327.87	30,499.89	–	419.70	23,826.54	6673.35
1-Octanol	–	277.77	332.63	30,063.43	–	414.87	24,103.94	5959.49
1-Heptanol	–	273.67	328.97	30,397.91	–	411.80	24,283.63	6114.28
1-Hexanol	–	268.77	327.95	30,492.45	–	405.36	24,669.43	5823.02
1-Butanol	240.10	279.60	331.90	30,129.56	–	372.30	26,860.06	3269.5
iso-Butanol	–	270.75	327.95	30,492.45	–	399.95	25,003.13	5489.32
2-Propanol	–	277.02	330.19	30,285.59	–	410.19	24,378.95	5906.64
Acetone	–	–	344.48	29,029.26	–	414.26	24,139.43	4889.83
1-Propanol	–	277.77	331.46	30,169.55	–	414.87	24,103.94	6065.61
Ethanol	–	278.94	327.87	30,499.89	–	410.19	24,378.95	6120.94
Benzonitrile	–	–	340.97	29,328.09	–	386.20	25,893.32	3434.77
Methanol	–	277.62	330.95	30,216.04	–	412.53	24,240.66	5975.38
DMF	–	–	331.46	30,169.55	–	419.70	23,826.54	6343.01
Acetonitrile	231.25	277.62	328.97	30,397.91	–	411.80	24,283.63	6114.28
Ethylene glycol	–	280.28	329.31	30,366.52	–	403.02	24,812.66	5553.86
DMSO	–	274.18	319.54	31,294.99	–	398.19	25,113.64	6181.35

315 nm, and 337–350 nm, respectively. The first transition band is just observed in polar protic solvents. The second transition band can represent the electronic transitions that originated from conjugation in the benzene ring. The third transition band is originated from conjugation between benzene rings and –N=CH– group.

The fluorescence spectra of S4 in different solvents are given in Table 4 and Fig. 5. As can be seen in Table 4 and Fig. 5 in the fluorescence spectra of S4, one band was observed. This band can represent the fluorescence transitions that originated from conjugation in –N=CH– group.

Solvatochromism

It is well known that solvent induces the spectral shift and related electronic transitions in the molecules. These spectral shifts are analyzed by using linear salvation energy relationships described with Kamlet–Taft and Catalan methods. Statistical parameters derived from maximum absorption and emission spectra are listed in Tables 5 and 6, respectively.

Figures 5S, 9S, 13S, and 17S show the correlation graph between the frequencies obtained experimentally using the Kamlet–Taft parameters for absorbance spectra S1, S2, S3, and S4 ($R^2 = 0.887$ (S1), $R^2 = 0.814$ (S2), $R^2 = 0.744$ (S3), and $R^2 = 0.627$ (S4)).

When the Kamlet–Taft parameters obtained by using the absorbance spectra of molecules are examined, it can be seen that the greatest contribution to absorbance spectra of S1, S2, S3, and S4 molecules is from the diffraction function. The Kamlet–Taft parameter calculations for maximum electronic absorption transition of S1, S2, S3, and S4 molecules are performed by using 27, 23, 23, and 22 solvents, respectively.

As seen from Table 5, C_1 is negative for all of the molecules and C_2 is negative for S3 and S4. It is found that $|C_1| > |C_2|$ for studied compounds. C_1 is a measurement of the orientation-induction interaction (refractive index function), while C_2 describes the dispersion-polarization

Table 4 The absorption and fluorescence wavenumber data in different solvent medium of S4 molecule

Solvents	$\lambda_{abs}{}^{1}$	$\lambda_{abs}{}^{2}$	$\lambda_{abs}{}^{3}$	$\lambda_{abs}{}^{4}$	$\nu_{abs}{}^{4}$	λ_{PL}	ν_{PL}	$\nu_{abs}4$-ν_{PL}
n-Pentane	–	264.98	305.61	–	–	405.95	24,633.58	–
n-Hexane	–	266.74	303.98	–	–	382.25	26,160.89	–
Cyclohexane	–	266.74	307.37	–	–	382.25	26,160.89	–
1,4-Dioxane	–	278.53	–	344.48	29,029.26	409.90	24,396.19	4633.07
Benzene	–	–	315.77	339.47	29,457.68	386.20	25,893.32	3564.36
Toluene	–	–	314.14	344.48	29,029.26	409.90	24,396.19	4633.07
o-Xylene	–	–	–	337.71	29,611.2	381.52	26,210.95	3400.25
Diethyl ether	–	276.87	–	341.10	29,316.92	409.90	24,396.19	4920.73
Chloroform	–	278.53	–	342.85	29,167.27	425.69	23,491.27	5676
Ethyl acetate	–	275.14	314.14	339.48	29,456.82	429.64	23,275.3	6181.52
n-Butyl acetate	–	278.53	–	346.24	28,881.7	386.20	25,893.32	2988.38
THF	–	279.03	–	344.48	29,029.26	386.20	25,893.32	3135.94
DCM	–	276.90	–	337.71	29,611.2	424.38	23,563.79	6047.41
1-Octanol	–	281.16	–	344.48	29,029.26	417.21	23,968.74	5060.52
1-Heptanol	223.85	275.14	–	346.24	28,881.7	410.19	24,378.95	4502.75
1-Hexanol	224.36	278.53	–	349.62	28,602.48	410.19	24,378.95	4223.53
1-Butanol	–	278.53	–	346.24	28,881.7	388.10	25,766.56	3115.14
iso-Butanol	–	276.90	–	339.47	29,457.68	400.53	24,966.92	4490.76
2-Propanol	–	278.53	–	341.10	29,316.92	384.15	26,031.5	3285.42
Acetone	–	–	–	353.01	28,327.81	417.21	23,968.74	4359.07
1-Propanol	–	278.53	–	344.48	29,029.26	425.69	23,491.27	5537.99
Ethanol	227.74	276.90	–	341.10	29,316.92	412.53	24,240.66	5076.26
Benzonitrile	–	–	317.90	–	–	381.52	26,210.95	–
Methanol	232.89	278.52	–	341.10	29,316.92	386.20	25,893.32	3423.6
DMF	–	–	–	344.48	29,029.26	386.02	25,905.39	3123.87
Acetonitrile	–	273.51	–	341.10	29,316.92	386.20	25,893.32	3423.6
Ethylene glycol	232.89	280.29	–	337.71	29,611.2	398.19	25,113.64	4497.56
DMSO	–	279.03	–	350.63	28,520.09	413.85	24,163.34	4357.09

(dielectric function). The values in Table 5 indicate that electronic transitions exhibit bathochromic effect (red shift) depending on dispersion-polarization force and the contribution of the dispersion-polarization force is greater than those of the orientation-induction force.

$|C_3|$ value is bigger than $|C_4|$ value for S1 and S4 molecules. Thus, electronic transitions of S1 and S4 molecules have occurred by the larger effect of H-bond acceptor ability in accordance with H-bond donor ability. However, H-bond donor ability in S2 and S3 molecules has a larger effect on electronic transition than H-bond acceptor ability.

Figures 6S, 10S, 14S, and 18S show the correlation graph between the frequencies obtained experimentally using the Kamlet–Taft parameters for fluorescence spectra of S1, S2, S3, and S4 ($R^2 = 0.738$, $R^2 = 0.753$, $R^2 = 0.837$, and $R^2 = 0.723$).

When the Kamlet–Taft parameters obtained by using the fluorescence spectra of molecules are examined, it can be seen that the greatest contribution to fluorescence spectra of S1, S2, S3, and S4 molecules is from the diffraction function (dispersion-induction interaction).

The Kamlet–Taft parameter calculations for maximum electronic emission transition of S1, S2, S3, and S4 molecules are performed by using 23, 24, 22, and 16 solvents, respectively. R^2 and R values given in Table 6 indicate acceptability of statistical parameters of the investigated molecules.

It can be said from Table 5 that absolute C_1 values derived from Kamlet–Taft model are obtained as bigger than C_2 values. Thus, electronic emission transitions are found more effective on dispersion-polarization interactions in comparison with orientation-induction interactions. Positive C_1 values show that electronic transitions in all molecules exhibit hypsochromic effect (blue shift) by the effect of dispersion-polarization forces. It is also observed that $|C_3| > |C_4|$ except for S1. Thus, the contribution of H-bond acceptor ability to the spectral shift in the electronic emission transitions in S2, S3, and S4 molecules is more effective than the contribution of H-bond donor ability. However, the inverse case is true for S1.

C_3 value is negative for S2 and S4 molecules, and this value is positive for S1 and S3 molecules. We can say that electronic emission spectra of S2 and S4 molecules exhibit red

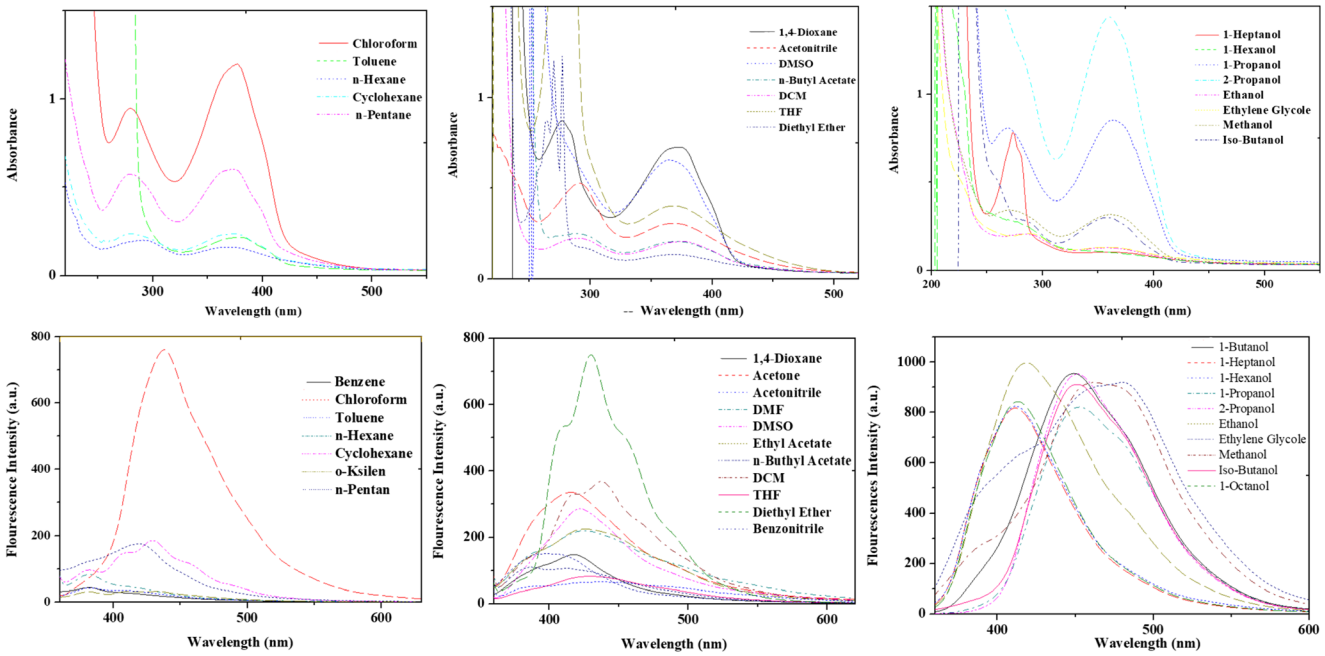

Fig. 2 The absorbance spectra and flourescence spectra of S1 molecule in the various solvents versus the wavelength (excitation wavelength is 340 nm)

shifts depending on H-bond acceptor ability of using solvents, while electronic emission spectra of S1 and S3 exhibit blue shifts depending on H-bond acceptor ability of solvents.

Figures 7S, 11S, 15S, and 19S show the correlation graph between the frequencies obtained experimentally using the Catalan parameters for absorbance spectra of S1, S2, S3, and S4 ($R^2 = 0.888$ (S1), $R^2 = 0.715$ (S2), $R^2 = 0.766$ (S3), and $R^2 = 0.729$ (S4)).

When the Catalan parameters obtained by using the absorbance spectra of molecules are examined, it can be seen that the greatest contribution to S1, S2, S3, and S4 molecules is from the solvent polarity (*SP*). The Catalan parameter calculations for maximum electronic absorption transition of S1 molecules have been carried out by using 28 solvents, while calculations for maximum electronic absorption transition of S2, S3, and S4 molecules are performed in 24, 25, and 26

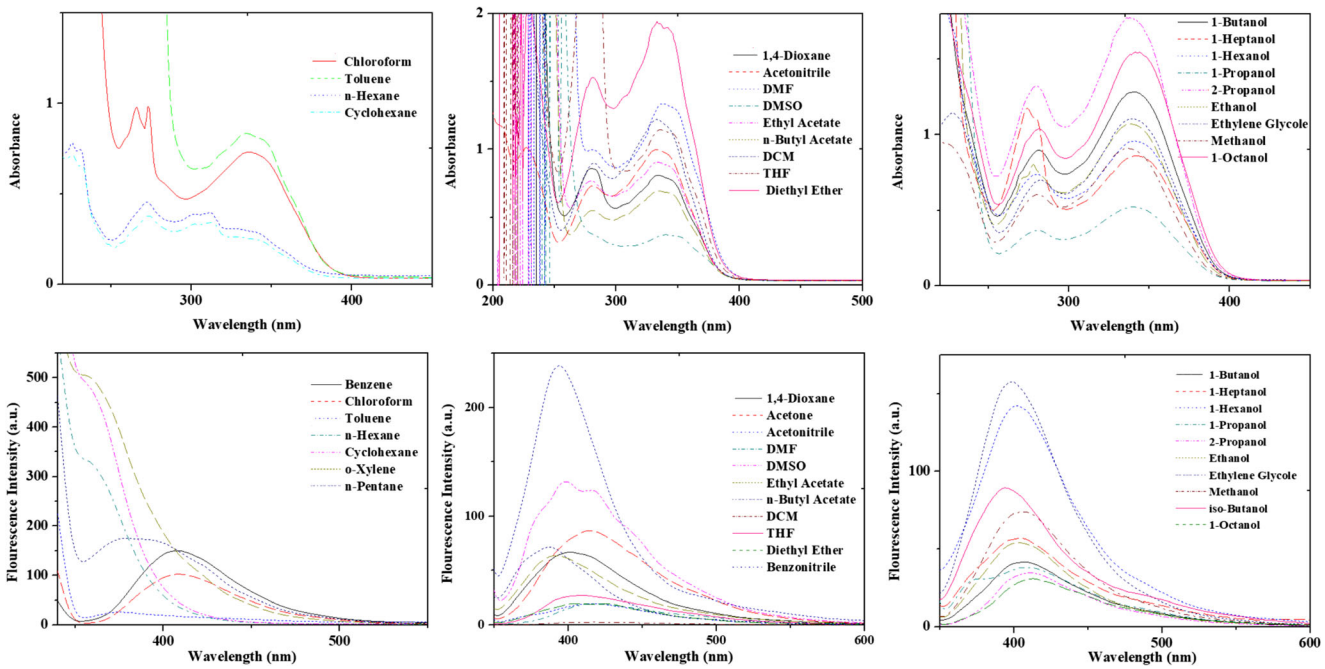

Fig. 3 The absorbance spectra and flourescence spectra of S2 molecule in the various solvents versus the wavelength (excitation wavelength is 330 nm)

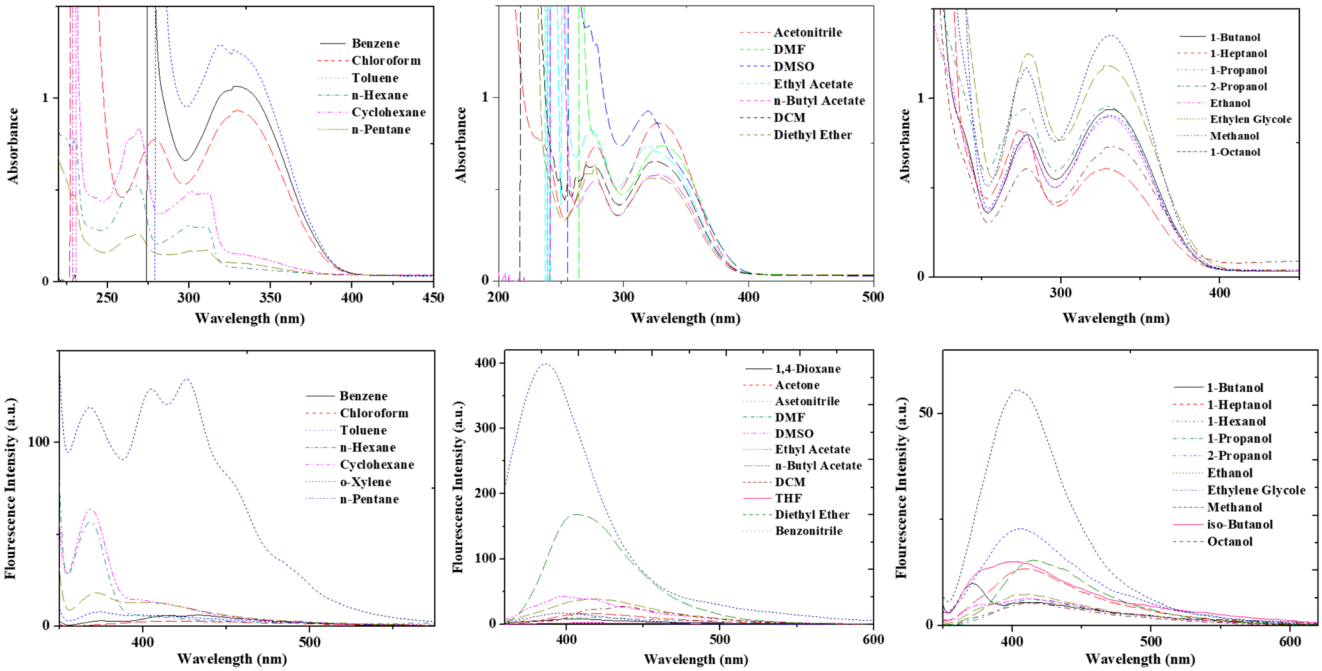

Fig. 4 The absorbance spectra and flourescence spectra of S3 molecule in the various solvents versus the wavelength (excitation wavelength is 330 nm)

solvents, respectively. According to MLRA results, polarity/polarizability of the solvent, C_6 coefficients are obtained as negative for all investigated molecules. This demonstrates that electronic absorption band maxima of S1, S2, S3, and S4 molecules exhibit bathochromic shift with increasing of polarity/polarizability of solvents. The coefficients C_8 and C_9 describe the contribution of solvent acidity (*SA*) and solvent basicity (*SB*) to the electronic absorption spectral shift, respectively. Negatively signed C_9 suggests that basicity of the solvent causes the absorption band shifts to lower energies with the increasing of solvent basicity for S2, S3, and S4. An inverse case for positively signed C_9 can be considered for S1 molecule.

According to the Catalan solvatochromic model, we have observed that $|C_8| > |C_9|$ for S1 and S2, whereas $|C_9| > |C_8|$ for S3 an S4. We can say that acidity of solvent is relatively more effective than basicity of solvent for S1 and S2. The inverse case can be considered for S3 and S4 molecules.

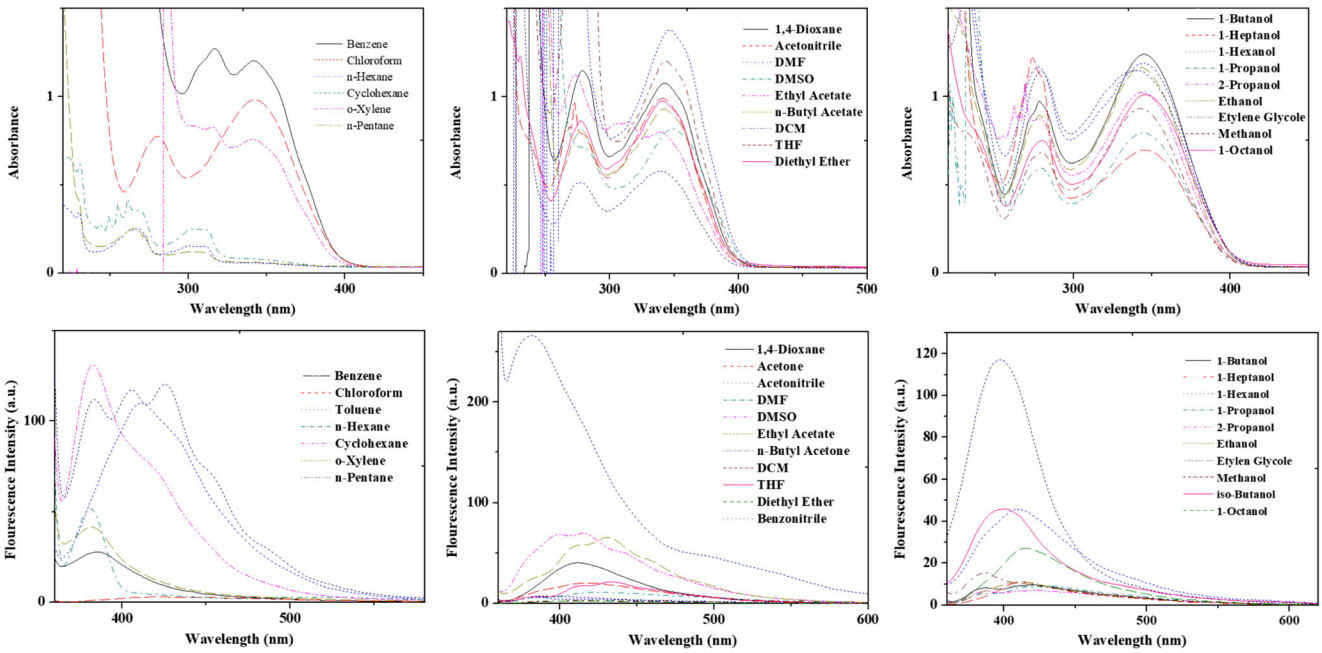

Fig. 5 The absorbance spectra and flourescence spectra of S4 molecule in the various solvents versus the wavelength (excitation wavelength is 340 nm)

Table 5 LSER's results calculated with using Kamlet–Taft and Catalan parameters for absorption maximum wavenumber of S1, S2, S3, and S4 molecules

Molecules	C_0	C_1	C_2	C_3		R	R^2	F	P	N	Extracted solvents
Kamlet–Taft solvatochromism (absorbance spectra)											
S1	26,590.92	−88.82	1031.87	399.32		0.920	0.847	42.29	0.000	27	–
S2	29,853.31	120.04	−85.63	−528.45		0.85	0.723	15.664	0.000	22	n-Pentane, n-Hexane, Toluene, o-Xylene, Benzonitrile, Acetonitrile
S3	32,215.11	−2453.96	−744.70	11.80		0.849	0.721	17.201	0.000	24	o-Xylene, 1-Octanol, Acetone, DMSO
S4	31,708.18	−3091.57	−1518.47	91.63		0.862	0.743	20.277	0.000	25	Ethyl acetate, Benzonitrile, Ethylene glycol
Molecules	C_4	C_5	C_6	C_7	C_8	R	R^2	F	P	N	Extracted solvents
Catalan solvatochromism (absorbance spectra)											
S1	27,484.05	−1482.01	396.12	1039.58	717.19	0.943	0.888	43.819	0.000	28	–
S2	30,960.25	−1868.35	512.80	−1250.54	−257.93	0.845	0.715	11.897	0.000	24	n-Pentane, n-Hexane, 1,4-Dioxane, Ethylene glycol
S3	34,964.56	−3685.91	−2207.07	927.25	−1282.07	0.875	0.766	16.400	0.000	25	Benzene, Toluene, DMSO
S4	36,160.51	−6689.20	−1904.59	1423.26	−2222.73	0.854	0.729	14.098	0.000	26	Ethyl acetate, Benzonitrile

Figures 8S, 12S, 16S, and 20S show the correlation graph between the frequencies obtained experimentally using the Catalan parameters for fluorescence spectra S1, S2, S3, and S4 ($R^2 = 0.759$ (S1), $R^2 = 0.712$ (S2), $R^2 = 0.736$ (S3), and $R^2 = 0.764$ (S4)). When the Catalan parameters obtained by using the fluorescence spectra of molecules are examined, it can be seen that the greatest contribution to S1 is from the solvent polarity (*SP*), to S2 and S3 from the solvent dipolarity (*SdP*), and to S4 from the solvent acidity (*SA*). The Catalan parameter calculations for maximum electronic emission transition of S1 molecule have been carried out by using 25 solvents, while calculations for maximum electronic absorption transitions of S2, S3, and S4 molecules are

Table 6 LSER's results calculated with using Kamlet–Taft and Catalan parameters for fluorescence maximum wavenumber of S1, S2, S3, and S4 molecules

Molecules	C_0	C_1	C_2	C_3		R	R^2	F	P	N	Extracted solvents
Kamlet–Taft solvatochromism (emission spectra)											
S1	26,611.75	−1852.31	−1261.67	−2358.82		0.846	0.715	15.066	0.000	22	n-Pentane, 1,4-Dioxane, Chloroform, Ethyl acetate, THF, Ethanol
S2	27,299.27	−3769.73	−1036.83	−59.93		0.861	0.741	17.172	0.000	22	n-Pentane, o-Xylene, 1-Propanol, Benzonitrile, Ethylene glycol, DMSO
S3	26,885.88	−223.58	−4075.86	1186.74		0.862	0.743	16.401	0.000	21	n-Pentane, Benzene, Chloroform, Ethyl acetate, DCM, 1-Butanol, DMSO
S4	26,133.35	1363.98	−2790.03	284.13		0.839	0.705	7.156	0.009	13	n-Pentane, 1,4-Dioxane, Benzene, Toluene, Chloroform, Ethyl acetate, DCM,1-Octanol, 1-Butanol, DMF, DMSO, 2-Propanol, Acetone, 1-Propanol, Benzonitrile
Molecules	C_4	C_5	C_6	C_7	C_8	R	R^2	F	P	N	Extracted solvents
Catalan solvatochromism (emission spectra)											
S1	22,851.66	4751.70	−3109.85	−3363.18	69.28	0.871	0.759	15.761	0.000	25	n-Pentane, Ethanol, Acetonitrile
S2	27,435.57	−26.29	−3045.62	1464.24	−1486.48	0.844	0.712	11.722	0.000	24	Benzene,1-Propanol, Ethylene glycol, DMSO
S3	27,817.55	−1202.95	−2768.37	1382.50	−1551.83	0.858	0.736	12.529	0.000	23	n-Pentane, Benzene, 1-Butanol, Benzonitrile, DMSO
S4	23,481.26	3900.03	−2832.92	−4785.85	1138.42	0.874	0.764	7.273	0.007	14	n-Pentane, Benzene, Toluene, Chloroform, Ethyl acetate, 1-Butanol, iso-Butanol, 2-Propanol, Ethanol, Benzonitrile, Methanol, DMF, Acetonitrile, Ethyl acetate, Glycerol

Table 7 Spectral treatment of the Lippert–Mataga, Bakhshiev, modified Bilot–Kawski, and Reichardt correlation of investigated compounds

Equation	Slope	Intercept	Cor. (R^2)	Solvent used in correlation	*N*
S1					
Lippert–Mataga	$m_1 = 18{,}320$	409.1	0.9841	n-Hexane, Cyclohexane, Benzene, Toluene, Ethyl acetate, THF, 1-Butanol, iso-Butanol, 2-Propanol, 1-Propanol, Methanol	11
Bakhshiev	$m_2 = 6743.6$	216.27	0.9992	Benzene, Toluene, Diethyl ether, Ethyl acetate, THF, 1-Butanol, 1-Propanol, Methanol	8
Modified Bilot–Kawski	$m_3 = -6897.7$	29,349	0.8522	DCM, 1-Butanol, iso-Butanol, 2-Propanol, 1-Propanol, Methanol, Ethylene glycol	7
Reichardt	$m_R = 216.78$	59.693	0.5865	n-Hexane, Cyclohexane, Benzene, Toluene, n-Butyl acetate, DCM, 1-butanol, iso-Butanol, 2-Propanol, Acetone, 1-Propanol, Benzonitrile, Methanol, DMF, Ethylene glycol, DMSO	16
S2					
Lippert–Mataga	$m_1 = 15{,}536$	1148.7	0.9166	n-Hexane, o-Xylene, Ethyl acetate, n-Butyl acetate, THF, 1-Heptanol, 1-Hexanol, 1-Octanol, 1-Butanol, 2-Propanol, Acetone, Benzonitrile, DMF, Acetonitrile, DMSO	15
Bakhshiev	$m_2 = 5664.5$	1272.7	0.9713	n-Hexane, o-Xylene, Ethyl acetate, n-Butyl acetate,1-Octanol,1-Heptanol, 2-Propanol, Acetone, DMF, Acetonitrile	10
Modified Bilot–Kawski	$m_3 = -5949.8$	30,621	0.9061	Cyclohexane, o-Xylene, Ethyl acetate, n-Butyl acetate, THF, DCM, 1-Octanol, 1-Heptanol, 1-Hexanol, Acetone	10
Reichardt	$m_R = 10{,}753$	1989.2	0.91	n-Hexane, Cyclohexane, Toluene, Chloroform, Ethyl acetate, n-Butyl acetate, THF, DCM, Acetone, DMF, Acetonitrile	11
S3					
Lippert–Mataga	$m_1 = 13{,}553$	2181	0.9198	o-Xylene, 1-Hexaneol, iso-Butanol, 2-Propanol, 1-Propanol, Ethanol, Methanol, DMF, Acetonitrile, Ethylene glycol DMSO	11
Bakhshiev	$m_2 = 4612.4$	2231.3	0.9354	o-Xylene, 1-Hexanol, iso-Butanol, 2-Propanol, 1-Propanol, Ethanol, Methanol, DMF, Acetonitrile, Ethylene glycol, DMSO	11
Modified Bilot–Kawski	$m_3 = -7874.6$	31,960	0.9126	n-Hexane, Cyclohexane, Toluene, Ethyl acetate, n-Butyl acetate, THF, DCM, 1-Octanol, 1-Heptanol, 2-Propanol, Acetone, 1-Propanol, Methanol	13
Reichardt	$m_R = 3107.5$	4198.9	0.9609	Toluene,1-Octanol,1-Heptanol, 1-Hexanol, 2-Propanol, 1-Propanol, Ethanol	7
S4					
Lippert–Mataga	$m_1 = 8514.5$	3252.5	0.9737	o-Xylene, Diethyl ether, 1-Octanol, 1-Propanol, Benzonitrile	5
Bakhshiev	$m_2 = 1155.9$	3476.1	0.9425	Benzene, o-Xylene, 1-Hexanol, iso-Butanol, Acetone, Ethylene glycol, DMSO	7
Modified Bilot–Kawski	$m_3 = -6730.2$	30,826	0.9388	n-Pentane, n-Hexane, Cyclohexane, 1,4-Dioxane, Toluene	5
Reichardt	$m_R = 5486.7$	1829.4	0.9053	n-Butyl Acetate, THF,1-Octanol, 1-Heptanol, iso-Butanol, 1-Propanol	6

performed in 24, 23, and 14 solvents, respectively. According to MLRA results, polarity/polarizability of the solvent, C_6 coefficients are obtained as negative for S2 and S3 molecules and as positive for S1 and S4 (Table 6). This demonstrates that electronic absorption band maxima of S2 and S3 shift to lower energy

Table 8 Onsager radius, ground-state (μ_g) and excited-state (μ_e) dipole moments (in Debye)

Molecule	a_0 (Å)	μ_g [a]	μ_e^{L-M}	μ_e^{B}	μ_e^{M-B-K}	μ_e^{R}	$\left(\frac{\mu_e}{\mu_g}\right)$ [b]	μ_g (D) Theo.
S1	5.18	0.11	3.19	1.97	1.89	1.061	0.011	4.48
S2	5.20	0.22	15.00	9.14	9.14	6.79	0.024	4.34
S3	5.16	2.81	16.46	10.77	10.77	6.39	0.261	3.64
S4	5.36	0.037	11.48	4.255	10.18	5.07	0.706	4.00

$1D = 3.33564 \times 10^{-30}$ cm $= 10^{-18}$ esu.cm

[a] Calculated according to Eq. (10)

[b] Calculated according to Eq. (12)

L-M, Lippert–Mataga method; *B*, Bakhshiev method; *M-B-K*, modified Bilot–Kawski method; *R*, Reichardt method

a_0 (Å) and μ_g (D) Theo. in gaseous phase is calculation with DFT (B3LYP)/6-311G(d, p) level of theory

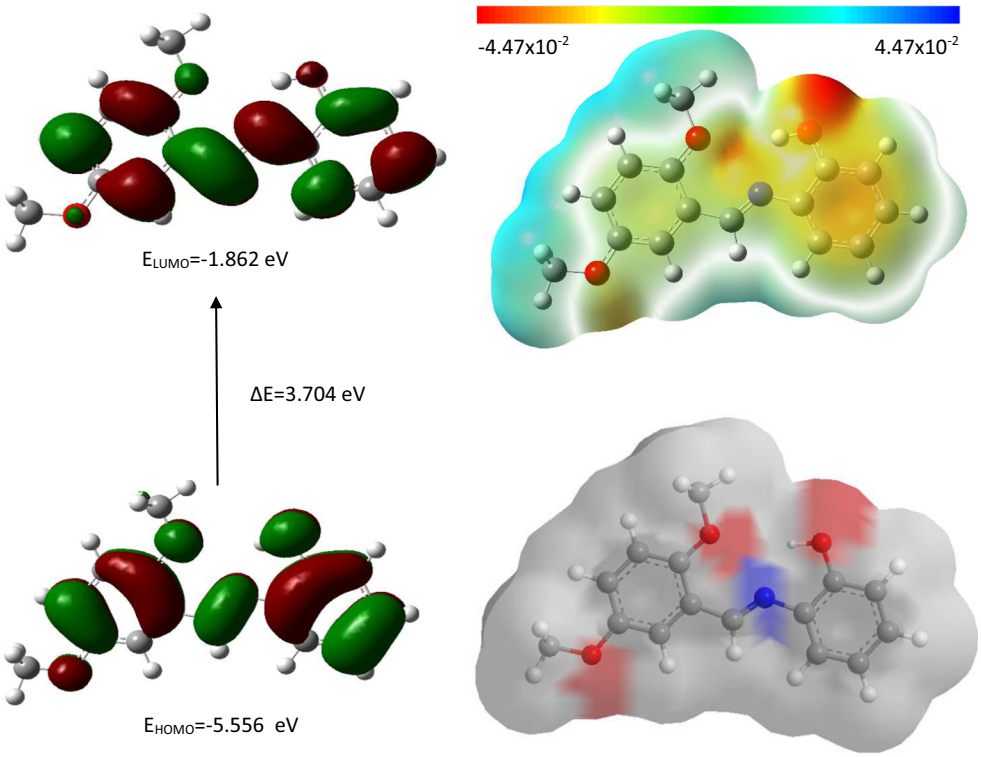

Fig. 6 HOMO, LUMO, MEP, and SAS shape of S1 molecule

exposing a bathochromic effect. However, polarity/polarizability of the solvent gives rise to a hypsochromic effect on these spectral shifts of S1 and S4.

According to the Catalan solvatochromic model, we have observed that $|C_8| > |C_9|$ for S1 and S4, whereas $|C_9| > |C_8|$ for S2 and S3. We can say that acidity of solvent is relatively more effective on electronic transitions than basicity of solvent for S1 and S4. We can say also that basicity of solvent is relatively more effective on electronic transitions than acidity of solvent for S2 and S3 (Table 6).

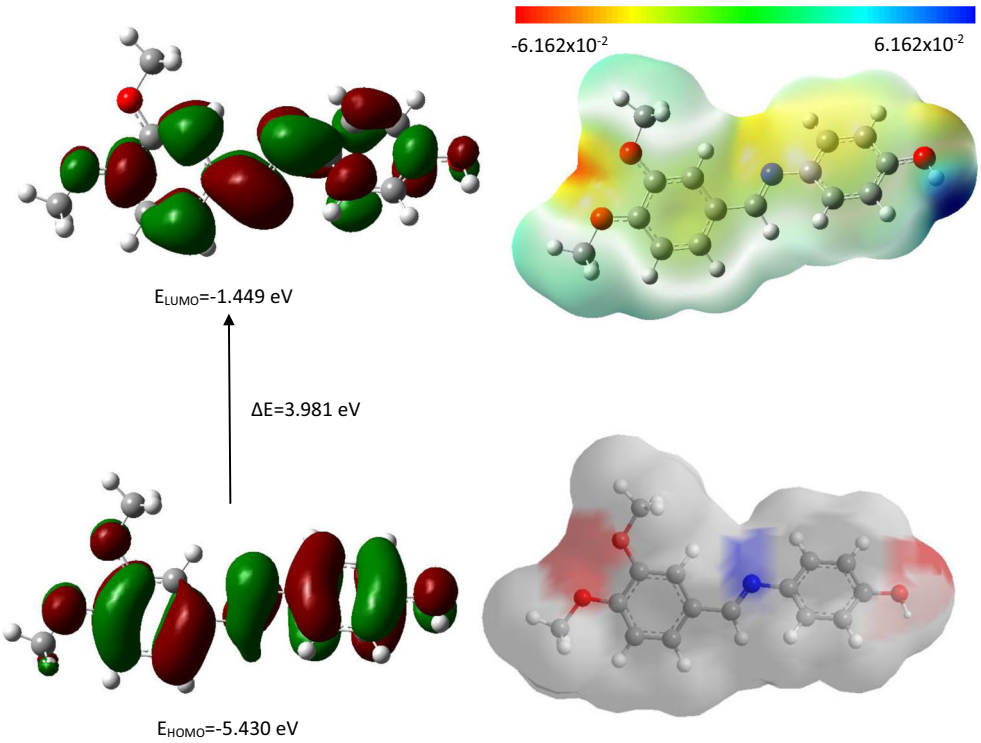

Fig. 7 HOMO, LUMO, MEP, and SAS shape of S2 molecule

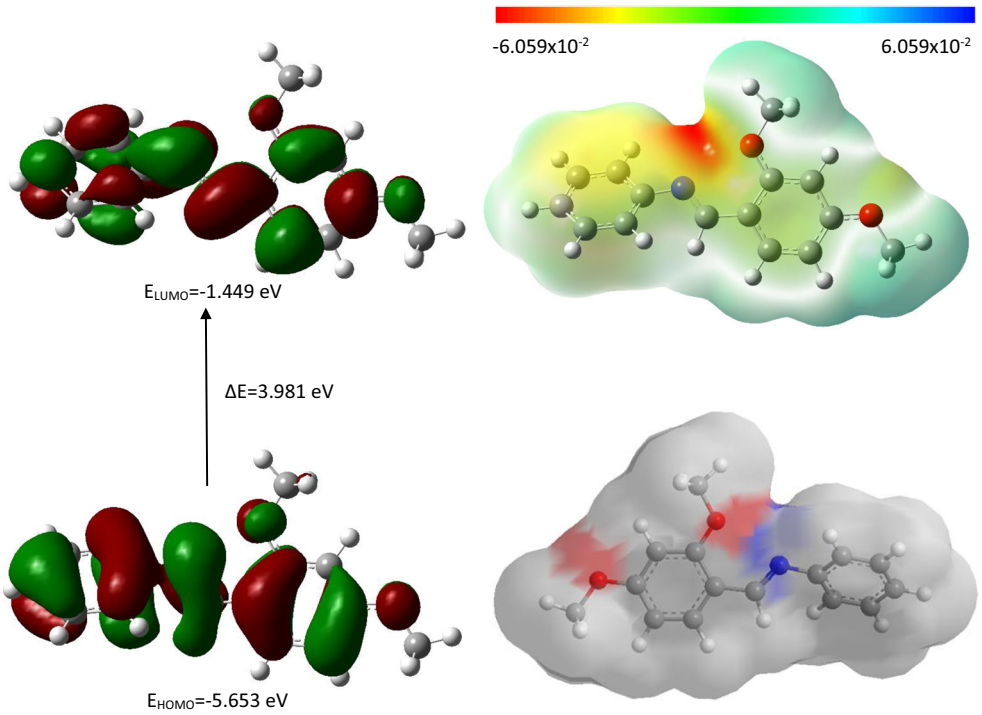

Fig. 8 HOMO, LUMO, MEP, and SAS shape of S3 molecule

Electrical dipole moments

Onsager cavity radius values are a_o=5.18A^0, a_o= 5.20A^0,a_o = 5.16 A^0, and a_o = 5.36 A^0 for S1, S2, S3, and S4, respectively, and these values are computed via using DFT-B3LYP/6-311G(d,p) method. Onsager cavity radius and dipole moments (Debye) calculated for investigated molecules at the ground- and excited-states are shown in Table 7.

Excited-state and ground-state dipole moments of investigated molecules were calculated by Lippert–Mataga,

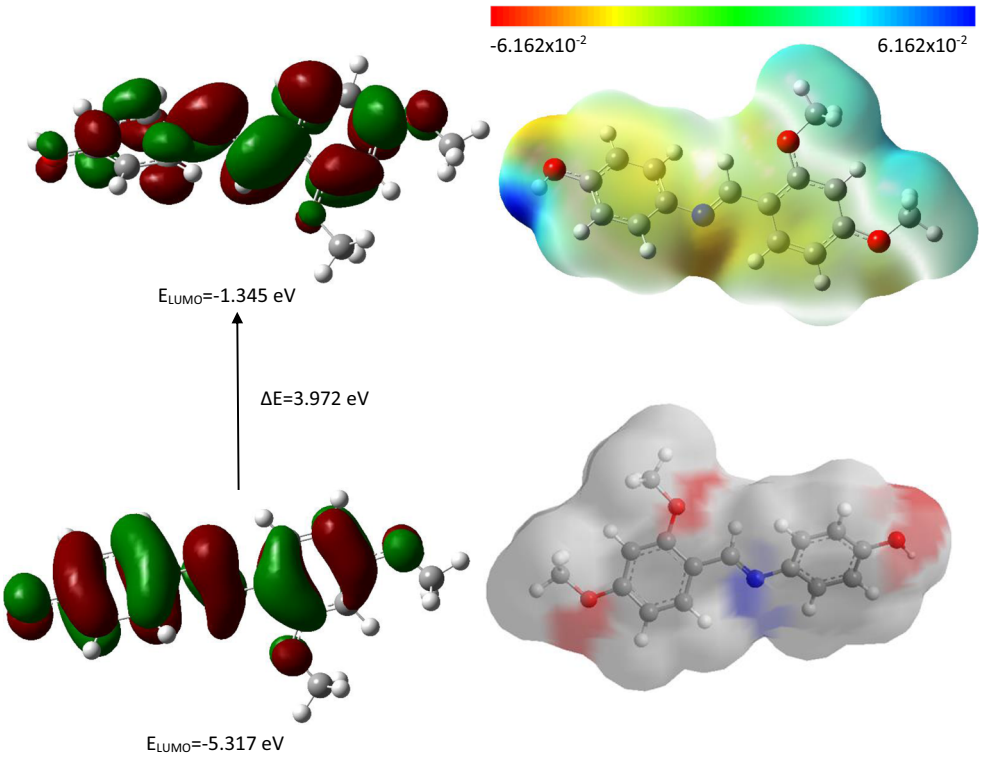

Fig. 9 HOMO, LUMO, MEP, and SAS shape of S4 molecule

Bakhshiev, and modified Bilot–Kawski methods. The results obtained in the calculations are as stated: In the ground-state, dipole moments for S1, S2, S3, and S4 are $\mu_g = 0.11\ D$, $\mu_g = 0.22\ D$, $\mu_g = 2.81\ D$, and $\mu_g = 0.037\ D$, respectively. In the excited-state, the dipole moments calculated by Lippert–Mataga method for S1, S2, S3, and S4 were found as $\mu_{e(L-M)} = 3.19$ D, $\mu_{e(L-M)} = 15$ D, $\mu_{e(L-M)} = 16.46$ D, and $\mu_{e(L-M)} = 11.48$, respectively. According to Bakhshiev method, excited-state electric dipole moment was found as $\mu_{e(B)} = 1.97$ D for S1, $\mu_{e(B)} = 9.14$ for S2, $\mu_{e(B)} = 10.77$ D for S3, and $\mu_{e(B)} = 4.255\ D$ for S4 molecule.

In the excited-state, the dipole moments calculated by modified Bilot-Kawski methods for S1, S2, S3, and S4 are $\mu_{e(M-B-K)} = 1.89\ D$, $\mu_{e(M-B-K)} = 9.14\ D$, $\mu_{e(M-B-K)} = 10.77\ D$, and $\mu_{e(M-B-K)} = 10.18\ D$, respectively. Furthermore, the dipole moments calculated by the Reichardt method for S1, S2, S3, and S4 in the excited-state are $\mu_{e(R)} = 1.061\ D$, $\mu_{e(R)} = 6.79\ D$, $\mu_{e(R)} = 6.39\ D$, and $\mu_{e(R)} = 5.07$ D, respectively. The correlation figures of the Lippert–Mataga, modified Bilot-Kawski, and Reichardt correlation spectral treatment of investigated molecules are shown in Table 8. For all cases, S1 has a smaller dipole moment in the excited-state. As seen in the table, the ratio of the excited-state dipole moments to the ground-state dipole moments is too great for all investigated molecules. So, we can say that charge irregularity is excessive in investigated molecules.

HOMO, LUMO, ΔE (E_{LUMO}-E_{HOMO}), MEP, and SAS shape

HOMO, LUMO, ΔE (E_{LUMO}-E_{HOMO}), MEP, and SAS shapes of investigated new Schiff bases molecules have been calculated by using DFT/B3LYP/6-311G(d,p) method and basis set in the gas phase and drawn to Figs. 6, 7, 8, and 9, respectively. The MEP shape shows to attemptable point interactions as electronic in the molecule. Thus, inasmuch as MEP figures, OH substituent of S1 molecule is acceptor site. The focus of having oxygen substituent in other molecules is electrophilic properties. As seen from Figs. 6, 7, 8, and 9, the blue color is methyl and hydrogen moiety of benzene rings, which is electropositive region. From MEP, S2 and S4 molecules have the highest electronegative and electropositive value. These regions can occur to electron transfer between solute with solvent molecule.

As seen from HOMO and LUMO shapes, the electron acceptor is in the red region, and the green regions are the electron donor regions, from where the possible electron transfer may be from where to the electron transfer during electronic excitation. Seen in ΔE, the lowest value has S1 molecule and the highest value has S2 and S3 molecules.

According to SAS images, the red and blue areas are areas where solvent interaction is possible. These regions are where oxygen and nitrogen atoms are present.

Conclusions

In this study,

- We have synthesized and characterized new Schiff base derivatives.
- These compounds have been commented in view of absorption and fluorescence electronic transitions.
- We have investigated the solvent effect on the electronic absorption bands for $\pi \rightarrow \pi^*$ and $n \rightarrow \pi^*$ electronic transitions.
- Solvent effect of Schiff base derivatives has been analyzed by Kamlet–Taft and Catalan approaches.
- We have calculated the ground-state electric dipole moment and excited-state electric dipole moment by using Lippert–Mataga, Bakhshiev, Kawski–Chamma–Viallet, and Reichardt solvatochromic shift methods.
- The excited-state dipole moment of G1, G2, and G3 is found to be larger than ground-state dipole moment by all of the methods.
- MEP, HOMO, LUMO, and SAS have been investigated theoretically.
- Excited- and ground-state charge distributions of the S4 molecule are found to be bigger than the other molecules.

Acknowledgements The authors greatly acknowledge the support of Bitlis Eren University, Scientific and Technological Application and Research Center. The authors greatly thank Bitlis Eren University for supporting this study by Gaussian 09 W and GaussView 5.0 software.

Funding information This work was financially supported by Bitlis Eren University Research Foundation. Project number: BEBAP-2014.05.

Compliance with ethical standards

Ethical statement/conflict of interest The authors declare that they have no conflict of interest.

References

1. da Silva CM, da Silva DL, Modolo LV, Alves RB, de Resende MA, Martins CVB et al (2011). J Adv Res 2(1):1–8
2. Schiff H (1866). Eur J Org Chem 140(1):92–137
3. Schiff H (1864). Ann Chem 131(1):118–119
4. Haas A, Lieb M, Schelvis M (1997). J Fluor Chem 83:133–143
5. Vaghasiya YK, Nair R, Soni M, Baluja S, Chanda S, Serb J (2004). Chem Soc 69:991–998
6. Arafath MA, Adam F, Al-Suede FSR, Razali MR, Ahamed MBK, Majid AMSA, Hassan MZ, Osman H, Abubakar S (2017, 1149). J Mol Struc:216–228
7. Neelima KP, Siddiqui S, Arshad M, Kumar D (2016). Spectr Acta Part A 155:146–154
8. Ganguly A, Chakraborty P, Banerjee K, Choudhuri SK (2014). Eur J Pharma Sci 51:96–109
9. Shanty AA, Mohanan PV (2018). Spectrochim Acta Part A 192: 181–187

10. Chithiraikumar S, Gandhimathi S, Neelakantan MA (2017). J of Mol Struct 1137:569–580
11. Zhang Y, Fang Y, Liang H, Wang H, Hu K, Liu X, Yi X, Peng Y (2013). Bioorg Med Chem Lett 23:107–111
12. Joshi R, Pandey N, Yadav SK, Tilak R, Mishra H, Pokharia S (2018). J Mol Struct 1164:386–403
13. Guo Z, Xing R, Liu S, Zhong Z, Ji X, Wanga L, Lia P (2007). Carbohydr Res 342:1329–1332
14. Parsaee Z, Mohammadi K (2017). J Mol Struct 1137:512–523
15. Tehrani KHME, Hashemi M, Hassan M, Kobarfard F, Mohebbi S (2016). Chin Chem Lett 27:221–225
16. Salehi M, Ghasemi F, Kubicki M, Asadi A, Behzad M, Ghasemi MH, Gholizadeh A (2016). Inorg Chim Acta 453:238–246
17. Dileepana AGB, Prakasha TD, Kumar GA, Shameela RP, Dhayabarana VV, Rajaram R (2018). J Photochem Photobiol B 183:191–200
18. Wang H, Yuan H, Li S, Li Z, Jiang M (2016). Bioorg Med Chem Lett 26:809–813
19. Sabaaa MW, Elzanaty AM, Abdel-Gawadb OF, Arafa EG (2018). Int J Biol Macromol 109:1280–1291
20. Ispir E, Toroğlu S, Kayraldız A (2008). Transit Met Chem 33:953–960
21. Kumar BNP, Mohana KN, Mallesha L (2013). J Fluor Chem 156: 15–20
22. Cheng L-X, Tang J-J, Luo H, Jin X-L, Dai F, Yang J, Qian Y-P, Li X-Z, Zhou B (2010). Bioorg Med Chem Lett 20:2417–2420
23. Sztanke K, Maziarka A, Osinka A, Sztanke M (2013). Bioorg Med Chem 21:3648–3666
24. Hranjec M, Starcevic K, Pavelic SK, Lucin P, Pavelic K, Zamola GK (2011). Eur J Med Chem 46:2274–2279
25. Jeevadason AW, Murugavel KK, Neelakantan MA (2014). Renew Sust Energ Rev 36:220–227
26. Panda U, Roy S, Mallick D, Layek A, Ray PP, Sinha C (2017). J Lumin 181:56–62
27. Zoubi WA, Mohanna NDA (2014). Spectrochim Acta A Mol Biomol Spectrosc 132:854–870
28. Singh AK, Gupta VK, Gupta B (2007). Anal Chim Acta 585:171–178
29. Gupta VK, Jain AK, Maheshwari G (2007). Talanta 72:49–53
30. Alizadeha K, Parooi R, Hashemi P, Rezaei B, Ganjali MR (2011). J Hazard Mater 186:1794–1800
31. Singh AK, Mehtab S (2008). Talanta 74:806–814
32. Ganjali MR, Tamaddon A, Norouzi P, Adib M (2006). Sensors Actuators B 120:194–199
33. Ganjali MR, Norouzi P, Daftari A, Faridbod F, Salavati-Niasari M (2007). Sensors Actuators B 120:673–678
34. Ganjali MR, Norouzi P, Faridbod F, Ghorbani M, Adib M (2006). Anal Chim Acta 569:35–41
35. Vijayalakshmi S, Kalyanaraman S (2013). Opt Mater 35:440–443
36. Shahid M, Salim M, Khalid M, Tahir MN, Khan MU, Brag AAC (2018). J Mol Struct 1161:66–75
37. Bhuiyan MDH, Teshome A, Gainsford GJ, Ashraf M, Clays K, Asselberghs I, Kay AJ (2010). Opt Mater 32:669–672
38. Jia J-H, Tao X-M, Li Y-J, Sheng W-J, Han L, Gao J-R, Zheng Y-F (2011). Chem Phys Lett 514:114–118
39. Vijayalakshmi S, Kalyanaraman S, Krishnakumar V (2013). Spectrochim Acta A 109:253–258
40. Wang K, Ma L, Liu G, Cao D, Guan R, Liu Z (2016). Dyes Pigments 126:104–109
41. Chalmardi GB, Tajbakhsh M, Hasani N, Bekhradnia A (2018). Tetrahedron 74:2251–2260
42. Sun C, Sun J, Che P, Chang Z, Li W, Qiu F (2017). J Lumin 188: 246–251
43. Jiaoa Y, Liua X, Zhoub L, He H, Zhoua P (2017). Duanb C Sensors and Actuators B 247:950–956
44. Singh TS, Paul PC, Pramanik HAR (2014). Spectrochim Acta A 121:520–526
45. Tajbakhsh M, Chalmardi GB, Bekhradnia A, Hosseinzadeh R, Hasani N, Amiri MA (2018). Spectrochim Acta A 189:22–31
46. Minkin VI, Tsukanov AV, Dubonosov AD, Bren VA (2011). J Mol Struct 998:179–191
47. Wang Q, Cai L, Gao F, Zhou Q, Zhan F, Wang Q (2010). J Mol Struct 977:274–278
48. Zhao L, Hou Q, Sui D, Wang Y, Jiang S (2007). Spectrochim Acta A 67:1120–1125
49. Liang Z, Liu Z, Gao Y (2007). Spectrochim Acta A 68:1231–1235
50. Gülseven Sıdır Y, Sıdır İ, Berber H, Türkoğlu G (2015). J Mol Liq 204:33–38
51. Payal R, Saroj MK, Sharma N, Rastog RC (2018). J Lumin 198:92–102
52. Sıdır İ, Gülseven Sıdır Y, Berber H, Türkoğlu G (2016). J Mol Liq 215:691–703
53. Gülseven Sıdır Y, Pirbudak G, Berber H, Sıdır İ (2017). J Mol Liq 242:1096–1110
54. Gülseven Sıdır Y, Sıdır İ, Berber H, Türkoğlu G (2014). J Mol Liq 199:57–66
55. Sıdır İ, Gülseven Sıdır Y, Berber H, Demiray F (2015). J Mol Liq 206:56–67
56. Wang W, Li R, Song T, Zhang C, Zhao Y (2016). Spectrochim Acta A 164:133–138
57. Yang Y-S, Ma S-S, Zhang Y-P, Ru J-X, Liu X-Y, Guo H-C (2018). Spectrochim Acta A 199:202–208
58. Gowda A, Roy A, Kumar S (2017). J Mol Liq 225:840–847
59. Liu Z, Zhang J, Li T, Yu Z, Zhang S (2013). J Fluor Chem 147:36–39
60. Rao GK, Kumar A, Singh MP, Kumar A, Biradar AM, Singh AK (2014). J Organomet Chem 753:42–47
61. Lippert E (1955). Z Naturforsch 10a:541–545
62. Mataga N, Kaifu Y, Koizumi M (1945). Bull Chem Soc Jpn 29: 465–470
63. Bakhshiev NG (1964). Opt Spektrosk 16:821–832
64. Reichardt C (1994). Chem Rev 94:2319–2358
65. Kawski A (1966). Acta Phys Pol 29:507–518
66. Kawski A (1992) Progress in photochemistry and photophysics. Boca Raton, Boston
67. Kawski A (2002). Z Naturforsch 57a:255–262
68. Kawski A (1964). Acta Phys Pol 25:285–290
69. Kawski A, Bojarski P, Kuklinski B (2008). Chem Phys Lett 463: 410–412
70. Kawski A (1992) in: J.F. Rabek (Ed.), Prog. Photochem. Photophys., vol. 5, CRC Press, Boca Raton, p. 1. Ann. Arbor, Boston
71. Chamma A, Viallet P (1970). C.R Acad Sci Paris Ser C 270:1901–1904
72. Kamlet MJ, Abboud JL, Abraham MH, Taft RW (1983). J Org Chem 48:2877–2887
73. Kamlet MJ, Abboud JL, Taft RW (1997). J Am Chem Soc 99(18): 6027–6038
74. Catalán J (2009). J Phys Chem B 113(17):5951–5960
75. Catalán J (2012). J Phys Chem A 116:4726–4794
76. Catalán J (2009). J Phys Chem B 113:5961–5960
77. Reichardt C (1982). in H. Ratajczak, W.J. Orville-Thomas (Eds), Molecular interactions, vol.3,John Wiley & Sons Ltd.
78. Reichardt C (2005). Solvents and solvent effects in organic chemistry. Third ed. Wiley-VCH, Weinheim Germany
79. Ravi M, Soujanya T, Samantha A, Radhakrishnan TP (1995). J Chem Soc Faraday Trans 91:2739–2742
80. Becke AD (1993). J Chem Phys 98:5648–5652
81. Frisch M J, Trucks G W, Schlegel H B, Scuseria G E, Robb M A, Cheeseman J R, Scalmani G, Barone V, Mennucci B, Petersson G A, Nakatsuji H, Caricato M, Li X, Hratchian H P, Izmaylov A F,

Bloino J, Zheng G, Sonnenberg J L, Hada M, Ehara M, Toyota K, Fukuda R, Hasegawa J, Ishida M, Nakajima T, Honda Y, Kitao O, Nakai H, Vreven T, Montgomery Jr JA, Peralta J E, Ogliaro F, Bearpark M, Heyd J J, Brothers E, Kudin K N, Staroverov V N, Kobayashi R, Normand J, Raghavachari K, Rendell A, Burant J C, Iyengar S S, Tomasi J, Cossi M, Rega N, Millam J M, Klene M, Knox J E, Cross J B, Bakken V, Adamo C, Jaramillo J, Gomperts R, Stratmann R E, Yazyev O, Austin A J, Cammi R, Pomelli C, Ochterski J W, Martin R L, Morokuma K, Zakrzewski V G, Voth G A, Salvador P, Dannenberg J J, Dapprich S, Daniels A D, Farkas O, Foresman J B, Ortiz J V, Cioslowski J, and Fox D J, Gaussian 09, Revision A.1 (Gaussian Inc., Wallingford, CT, 2009)

82. Dennington R, Keith T, Milam J, GaussView, Version 5, Semichem Inc., Shawnee Mission KS, 2009